

Symmetry fingerprints of a benzene single-electron transistor: Interplay between Coulomb interaction and orbital symmetry

Georg Begemann, Dana Darau, Andrea Donarini, and Milena Grifoni
Theoretische Physik, Universität Regensburg, 93040 Regensburg, Germany
 (Received 18 April 2008; published 29 May 2008)

The interplay between Coulomb interaction and orbital symmetry produces specific transport characteristics in molecular single electron transistors (SETs) that can be considered as the fingerprints of the contacted molecule. Specifically we predict, for a benzene SET, selective conductance suppression and the appearance of negative differential conductance when changing the contacts from para to meta configuration. Both effects originate from destructive interference in transport involving states with *orbital degeneracy*.

DOI: [10.1103/PhysRevB.77.201406](https://doi.org/10.1103/PhysRevB.77.201406)

PACS number(s): 85.65.+h, 73.63.-b

Understanding the conduction characteristics through single molecules is one of the crucial issues in molecular electronics.¹ The dynamics of the electron transfer to and from the molecule depends on the intrinsic electronic spectrum of the molecule as well as on the electronic coupling of the molecule to its surroundings.

In recent years, the measurement of stability diagrams of single electron transistor (SET) devices has become a very powerful tool to do spectroscopy of small conducting systems via transport experiments. Thus the capability to perform three terminal measurements on single molecules²⁻¹⁰ has been a fundamental achievement for molecular electronics. Such molecular transistors might display transport properties that are very different from those of conventional SETs. In fact, vibrational or torsional modes^{7,10} and intrinsic symmetries of the molecule can hinder or favor transport through the SET, visible, e.g., in the absence or presence of specific excitation lines in the stability diagram of the molecular SET, or in negative differential conductance features. Many-body phenomena such as, e.g., the Kondo effect, have been observed as well.^{2,3,5,10}

Despite the experimental progress, the theoretical understanding of the properties of single organic molecules coupled to electrodes is far from being satisfactory. On the one hand, numerical approaches to transport based, e.g., on the combination of Green's function methods with density-functional theory have become a standard approach to study transport at the nanoscale.¹ However, this technique is not appropriate for the description of transport through a molecule weakly coupled to leads, due to the crucial role played by the Coulomb interaction in these systems. Hence, in Ref. 11, an electronic structure calculation for a benzene molecule was performed in order to arrive at an effective interacting Hamiltonian for the π orbitals, to be solved to determine the I - V characteristics of a benzene junction.

In this paper, we consider the electronic transport through a benzene SET. Similar to Ref. 11, in order to devise a semi-quantitative description, we start from an interacting Hamiltonian of isolated benzene where only the localized p_z orbitals are considered and the ions are assumed to have the same spatial symmetry as the relevant electrons. The Hamiltonian for the isolated molecule possesses $4^6=4096$ eigenstates, to be calculated numerically, and whose symmetries can be established with the help of group theory. Large degeneracies

of the electronic states occur. For example, while the six-particle ground state (A_{1g} symmetry) is nondegenerate, there exist four seven-particle ground states due to spin and orbital (E_{2u} symmetry) degeneracy. When coupling the benzene SET to leads in the meta and para configurations (see Fig. 1), these orbital symmetries lead to very different stability diagrams for the two configurations (see Fig. 2). Striking are the selective reduction of conductance (Fig. 3) and the occurrence of negative differential conductance (NDC) features when changing from para to meta configuration. As shown in Fig. 4, the NDC effect occurs due to the formation of a blocking state at certain values of the bias voltage. The blocking is clearly visible by monitoring the position-dependent many-body transition probabilities, which, at given values of the bias voltage, can exhibit nodes at the same position as one of the contacts. NDC for benzene junctions has been predicted also in Ref. 11, but in the para configuration and *only* in the presence of a dissipative electromagnetic bath. In our work, NDC occurs despite the absence of the bath. Both of the effects we predict originate from bias-dependent interference of orbitally degenerate states: coherences, neglected in Ref. 11, are essential to capture interference effects when solving the equations for the benzene's occupation probabilities. Interference phenomena in transport through benzene have been recently discussed also in Refs. 12 and 13. The parameter regime is, however, very different, as both discuss the strong tunneling limit, where Coulomb blockade effects are not relevant.

We start from the total Hamiltonian $H=H_{\text{ben}}+H_{\text{leads}}+H_T$, where the Hamiltonian for benzene reads

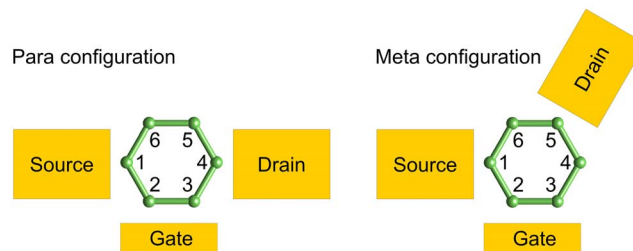


FIG. 1. (Color online) The two different setups for the benzene SET considered in this paper.

$$\begin{aligned}
H_{\text{ben}} = & \xi_0 \sum_{i\sigma} d_{i\sigma}^\dagger d_{i\sigma} + b \sum_{i\sigma} (d_{i\sigma}^\dagger d_{i+1\sigma} + d_{i+1\sigma}^\dagger d_{i\sigma}) \\
& + U \sum_i \left(n_{i\uparrow} - \frac{1}{2} \right) \left(n_{i\downarrow} - \frac{1}{2} \right) \\
& + V \sum_i (n_{i\uparrow} + n_{i\downarrow} - 1)(n_{i+1\uparrow} + n_{i+1\downarrow} - 1). \quad (1)
\end{aligned}$$

Here $d_{i\sigma}^\dagger$ creates an electron of spin σ in the p_z orbital of carbon i , $i=1, \dots, 6$ runs over the six carbon atoms of benzene and $n_{i\sigma} = d_{i\sigma}^\dagger d_{i\sigma}$. This Hamiltonian respects the D_{6h} symmetry of benzene and also the particle-hole symmetry. Mechanical oscillations at this level are neglected and all the atoms are considered in their equilibrium position. The parameters b , U , and V for isolated benzene are given in the literature¹⁴ and are chosen to fit excitation spectra. Even if the presence of metallic electrodes is expected to cause a substantial renormalization of U and V , we do not expect the main results of this work to be affected by this change. The weak coupling suggests that the symmetry of the molecule will remain unchanged and with it the structure of the Hamiltonian (1). The gate voltage V_g is introduced by a renormalized on-site energy $\xi = \xi_0 - eV_g$ and we conventionally set $V_g=0$ at the charge-neutrality point. We represent source and drain leads as two reservoirs of noninteracting electrons: $H_{\text{leads}} = \sum_{\alpha k \sigma} (\epsilon_k - \mu_\alpha) c_{\alpha k \sigma}^\dagger c_{\alpha k \sigma}$, where $\alpha=L, R$ and the chemical potentials μ_α of the leads depend on the applied bias voltage $\mu_{L,R} = \mu_0 \pm \frac{V_b}{2}$. In the following, we will measure the energy starting from the equilibrium chemical potential $\mu_0=0$. The coupling to source and drain leads is described by

$$H_T = t \sum_{\alpha k \sigma} (d_{\alpha \sigma}^\dagger c_{\alpha k \sigma} + c_{\alpha k \sigma}^\dagger d_{\alpha \sigma}), \quad (2)$$

where we define $d_{\alpha \sigma}^\dagger$ as the creator of the electron in the benzene carbon atom that is closest to the lead α . In particular, $d_{R\sigma}^\dagger := d_{4\sigma}^\dagger, d_{5\sigma}^\dagger$ in the para and meta configurations, respectively, while $d_{L\sigma}^\dagger := d_{1\sigma}^\dagger$ in both setups. Due to the weak coupling to the leads, we can assume that the potential drop is all concentrated at the lead-molecule interface and is not affecting the molecule itself. Given the high degeneracy of the spectrum, the method of choice to treat the dynamics in the weak coupling is the Liouville equation method already used, e.g., in Refs. 15 and 16. The starting point is the Liouville equation for the reduced density operator $\dot{\sigma} = \text{Tr}_{\text{leads}}\{\dot{\rho}\} = -\frac{i}{\hbar} \text{Tr}_{\text{leads}}\{[H, \rho]\}$, where ρ is the density operator.¹⁷ Due to the weak coupling to the leads, we treat the effects of H_T to the lowest nonvanishing order. The reduced density operator σ is defined on the Fock space of benzene, but coherences between states with different particle number and different energy can be neglected, the former because they are decoupled from the dynamics of the populations, the latter being irrelevant due to their fast fluctuation (secular approximation). As a result, we arrive at a generalized master equation (GME) where coherences between degenerate states are retained. This approach is robust against the small asymmetries introduced in the molecule by the coupling to the leads or by deformation as far as the energy splitting that lifts the orbital degeneracy is comparable to the thermal energy. In particu-

lar, the results presented in this paper are robust against the residual potential drop that even in weak coupling could affect the molecule itself. The GME is conveniently expressed in terms of the reduced density operator $\dot{\sigma}^{NE} = \mathcal{P}_{NE} \dot{\sigma} \mathcal{P}_{NE}$, where $\mathcal{P}_{NE} := \sum_{\ell\tau} |NE\ell\tau\rangle\langle NE\ell\tau|$ is the projection operator on the subspace of N particles and energy E . The sum runs over the orbital and spin quantum numbers ℓ and τ , respectively. Eventually the GME reads

$$\begin{aligned}
\dot{\sigma}^{NE} = & - \sum_{\alpha\tau} \frac{\Gamma_\alpha}{2} \left\{ d_{\alpha\tau} \left[f_\alpha^+(H_{\text{ben}} - E) + \frac{i}{\pi} p_\alpha(H_{\text{ben}} - E) \right] d_{\alpha\tau}^\dagger \sigma^{NE} \right. \\
& \left. + d_{\alpha\tau}^\dagger \left[f_\alpha^-(E - H_{\text{ben}}) - \frac{i}{\pi} p_\alpha(E - H_{\text{ben}}) \right] d_{\alpha\tau} \sigma^{NE} + \text{H.c.} \right\} \\
& + \sum_{\alpha\tau E'} \Gamma_\alpha \mathcal{P}_{NE} \{ d_{\alpha\tau}^\dagger f_\alpha^+(E - E') \sigma^{N-1E'} d_{\alpha\tau} \\
& + d_{\alpha\tau} f_\alpha^-(E' - E) \sigma^{N+1E'} d_{\alpha\tau}^\dagger \} \mathcal{P}_{NE}, \quad (3)
\end{aligned}$$

where $\Gamma_{L,R} = \frac{2\pi}{\hbar} |t_{L,R}|^2 \mathcal{D}_{L,R}$ is the bare transfer rates with the constant densities of states of the leads $\mathcal{D}_{L,R}$.

Terms describing sequential tunneling from and to the lead α are proportional to the Fermi function $f(x - \mu_\alpha) := f_\alpha^+(x)$ and $f_\alpha^-(x) = 1 - f_\alpha^+(x)$, respectively. Still in the sequential tunneling limit, but due to the presence of coherences, also energy nonconserving terms appear in the generalized master equation; they are proportional to the function $p_\alpha(x) = -\text{Re} \psi \left[\frac{1}{2} + \frac{i\beta}{2\pi} (x - \mu_\alpha) \right]$, where ψ is the digamma function.^{16,17} Finally, we write the GME on the basis of the energy eigenstates for isolated benzene and find numerically the stationary solution.

A closer analysis of the master equation allows us also to define a current operator (one per molecule-lead contact)

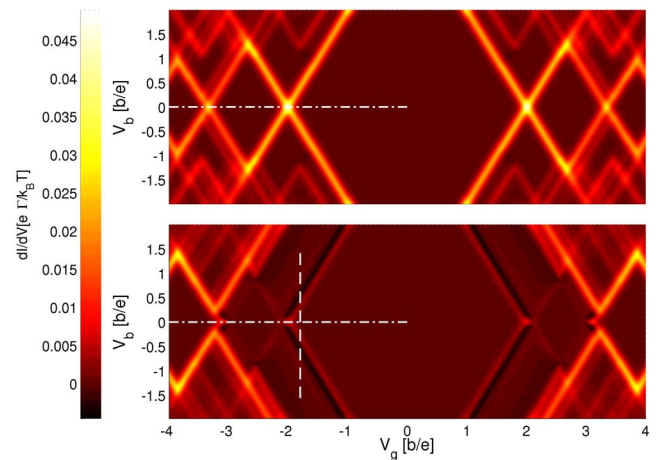


FIG. 2. (Color online) Stability diagram for the benzene SET connected in the para (above) and meta (below) configuration. White dot-dashed lines highlight the conductance cuts presented in Fig. 3; the white dashed line shows the region corresponding to the current trace presented in Fig. 4. The parameters used are $U=4|b|$, $V=2.4|b|$, $T=0.04|b|$, and $\Gamma=10^{-3}|b|$.

$$\hat{I}_\alpha = \sum_{NE\tau} \mathcal{P}_{NE} [d_{\alpha\tau} f_\alpha^+(H_{\text{ben}} - E) d_{\alpha\tau}^\dagger - d_{\alpha\tau}^\dagger f_\alpha^-(E - H_{\text{ben}}) d_{\alpha\tau}] \mathcal{P}_{NE} \quad (4)$$

and calculate the stationary current as the average $I_L = \text{Tr}\{\sigma_{\text{stat}} \hat{I}_L\} = -I_R$, with σ_{stat} the stationary density operator. In Fig. 2, we present the stability diagram for the benzene SET contacted in the para (upper panel) and meta position (lower panel). Bright ground-state transition lines delimit diamonds of zero differential conductance typical of the Coulomb blockade regime while a rich pattern of satellite lines represents the transitions between excited states. Though several differences can be noticed, most striking are the suppression of conductance and the appearance of NDC when passing from para to meta configuration.

A zero bias cut of the stability diagrams as a function of the gate voltage V_g is plotted in Fig. 3. Only transitions between lowest energy states are relevant for the conductance. The number of p_z electrons on the molecule and the symmetry of the many-body state corresponding to the conductance valleys are reported. The conductance in the meta and para configuration is the same for the $N=11 \leftrightarrow 12$ and $N=10 \leftrightarrow 11$ transitions, while it is systematically suppressed in all other cases. In other terms, transitions between states with A or B symmetry, which do not have orbital degeneracy, are invariant under configuration change; transitions that involve *both* of the orbitally degenerate E symmetry states are suppressed. *Destructive interference* between orbitally degenerate states explains the systematic conductance suppression. The eight-particle ground state is antisymmetric¹¹ (with respect to the plane through the contact atoms and perpendicular to the molecular plane), thus excluded from transport in the para configuration and replaced by the first excited symmetric E_{2g} state. This explains the peculiar position of the 7-8 and 8-9 resonances. By neglecting the energy noncon-

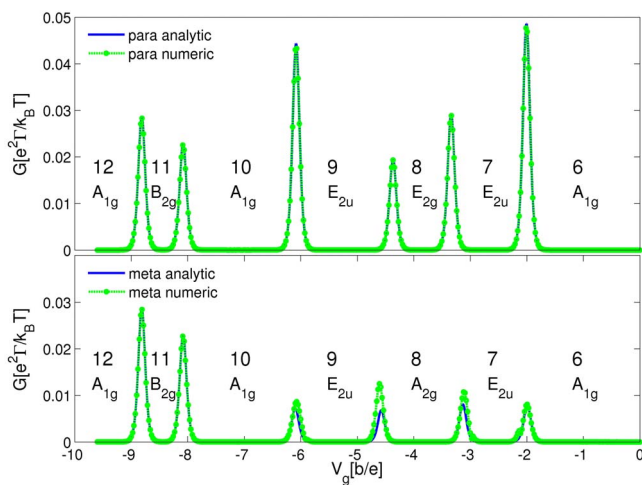


FIG. 3. (Color online) Conductance of the benzene SET as a function of the gate voltage in the para (above) and meta (below) configurations. In the low conductance valleys, the state of the system has a definite number of particles and symmetry as indicated. Selective conductance suppression when changing from the meta to the para configuration is observed.

serving terms in Eq. (3), we derived an analytical formula for the conductance close to the resonance between N and $N+1$ particle states,

$$G_{N,N+1}(\Delta E) = 2e^2 \frac{\Gamma_L \Gamma_R}{\Gamma_L + \Gamma_R} \frac{|\sum_{nm\tau} \langle N, n | d_{L\tau} | N+1, m \rangle \langle N+1, m | d_{R\tau}^\dagger | N, n \rangle|^2}{\sum_{nm\alpha\tau} |\langle N, n | d_{\alpha\tau} | N+1, m \rangle|^2} \times \left[-\frac{f'(\Delta E)}{(S_{N+1} - S_N) f(\Delta E) + S_N} \right], \quad (5)$$

where $\Delta E = E_{g,N} - E_{g,N+1} + eV_g$ is the energy difference between the benzene ground states with N and $N+1$ electrons diminished by a term linear in the side gate; n and m label the S_N -fold and S_{N+1} -fold degenerate ground states with N and $N+1$ particles, respectively. Interference effects are contained in the numerator of the third factor (overlap factor Λ). In order to make these more visible, we remind the reader that $d_{R\tau}^\dagger = \mathcal{R}_\phi^\dagger d_{L\tau}^\dagger \mathcal{R}_\phi$, where \mathcal{R}_ϕ is the rotation operator of an angle ϕ and $\phi = \pi$ for the para while $\phi = 2\pi/3$ for the meta configuration. All eigenstates of H_{ben} are eigenstates of the discrete rotation operators with angles multiples of $\pi/3$ and the eigenvalues are phase factors. The overlap factor now reads

$$\Lambda = \left| \sum_{nm\tau} |\langle N, n | d_{L\tau} | N+1, m \rangle|^2 e^{i\phi_{nm}} \right|^2, \quad (6)$$

where ϕ_{nm} encloses the phase factors coming from the rotation of the states $|N, n\rangle$ and $|N+1, m\rangle$. Interference is possible only when S_N or $S_{N+1} > 1$, that is, in the presence of degenerate states. It generates a considerable reduction by passing

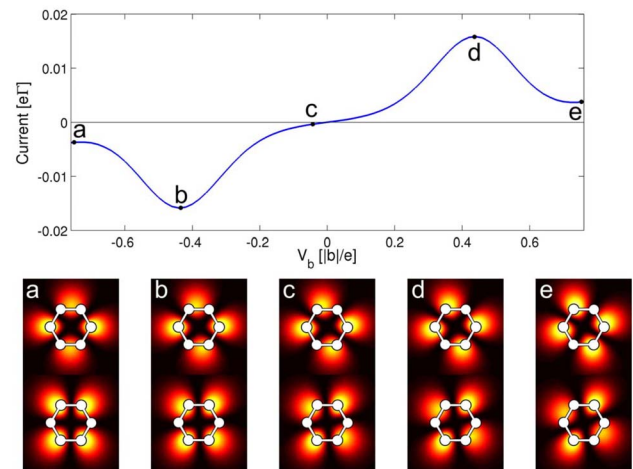


FIG. 4. (Color online) Upper panel: Current through the benzene SET in the meta configuration calculated at bias and gate voltage conditions indicated by the dashed line of Fig. 2. A pronounced NDC is visible. Lower panels: Transition probabilities between the six-particle and each of the two seven-particle ground states for bias voltage values labeled a - e in the upper panel. The transitions to a blocking state are visible in the upper (lower) part of the e (a) panels.

from the para to the meta configuration, as seen in Fig. 3.

Interference also affects nonlinear transport and produces in the meta configuration NDC at the border of the six-particle state diamond (Fig. 2). The upper panel of Fig. 4 shows the current through the benzene SET contacted in the meta configuration as a function of the bias voltage. The current is given for parameters corresponding to the white dashed line of Fig. 2. In this region, only the six- and seven-particle ground states are populated. The six-particle ground state is not degenerate. The seven-particle ground state is fourfold degenerate, although the twofold spin degeneracy is not important since spin coherences vanish in the stationary limit and the $S_z = \frac{1}{2}$ and $-\frac{1}{2}$ density matrices are equal for symmetry. At low bias, the six-particle state is mainly occupied. As the bias is raised, transitions $6 \leftrightarrow 7$ occur and current flows. Above a certain bias threshold, a blocking state is populated and the current is reduced. To visualize this, we introduce the probability (averaged over the z coordinate and the spin σ)

$$P(x, y; \ell \tau) = \lim_{L \rightarrow \infty} \sum_{\sigma} \frac{1}{2L} \int_{-L/2}^{L/2} dz |\langle 7g \ell \tau | \psi_{\sigma}^{\dagger}(\vec{r}) | 6g \rangle|^2 \quad (7)$$

for benzene to make a transition between the state $|6g\rangle$ and one of the states $|7g \ell \tau\rangle$ by adding or removing an electron in

position \vec{r} and spin σ . Each of the lower panels of Fig. 4 is a surface plot of $P(x, y; \ell \tau)$ for the seven-particle basis that diagonalizes the stationary density matrix at a fixed bias. The upper plot of the e panel describes the transitions to the blocking seven-particle state that accepts electrons from the source lead (close to carbon 1) but cannot release electrons to the drain (close to carbon 5). The energy nonconserving rates prevent the complete efficiency of the blocking by ensuring a slow depopulation of the blocking state. At large negative bias, the blocking scenario is depicted in panel a . We remark that only a description that retains coherences between the degenerate seven-particle ground states correctly captures NDC at both positive and negative bias.

To summarize, we analyzed the transport characteristics of a benzene-based SET. The interplay between Coulomb interaction and orbital symmetry is manifested in a destructive interference involving orbitally degenerate states, leading to selective conductance suppression and negative differential conductance when changing the contacts from para to meta configuration.

We acknowledge financial support from the DFG within the research programs SPP 1243 and SFB 689.

-
- ¹ *Introducing Molecular Electronics*, edited by G. Cuniberti, G. Fagas, and K. Richter (Springer, Berlin, 2005).
- ² J. Park, A. N. Pasupathy, J. I. Goldsmith, C. Chang, Yu. Yaish, J. R. Petta, M. Rinkoski, J. P. Sethna, H. D. Abruna, P. L. McEuen, and D. C. Ralph, *Nature* **417**, 722 (2002).
- ³ W. Liang, M. P. Shores, M. Bockrath, J. R. Long, and H. Park, *Nature* **417**, 725 (2002).
- ⁴ S. Kubatkin, A. Danilov, M. Hjort, J. Cornil, J.-L. Brédas, N. Stuhr-Hansen, P. Hedegård, and T. Bjørnholm, *Nature* **425**, 698 (2003).
- ⁵ L. H. Yu, Z. K. Keane, J. W. Cizek, L. Cheng, J. M. Tour, T. Baruah, M. R. Pederson, and D. Natelson, *Phys. Rev. Lett.* **95**, 256803 (2005).
- ⁶ A. V. Danilov, S. Kubatkin, S. Kafanov, P. Hedegård, N. Stuhr-Hansen, K. Moth-Poulsen, and T. Bjørnholm, *Nano Lett.* **8**, 1 (2008).
- ⁷ D.-H. Chae, J. F. Berry, S. Jung, F. A. Cotton, C. A. Murillo, and Z. Yao, *Nano Lett.* **6**, 165 (2006).
- ⁸ M. Poot, E. Osorio, K. O'Neill, J. M. Thijssen, D. Vanmaekelbergh, C. A. van Walree, L. W. Jenneskens, and H. S. J. van der Zant, *Nano Lett.* **6**, 1031 (2006).
- ⁹ H. B. Heersche, Z. de Groot, J. A. Folk, H. S. J. van der Zant, C. Romeike, M. R. Wegewijs, L. Zobbi, D. Barreca, E. Tondello, and A. Cornia, *Phys. Rev. Lett.* **96**, 206801 (2006).
- ¹⁰ E. A. Osorio, K. O'Neill, N. Stuhr-Hansen, O. F. Nielsen, T. Bjørnholm, and H. S. J. van der Zant, *Adv. Mater. (Weinheim, Ger.)* **19**, 281 (2007).
- ¹¹ M. H. Hettler, W. Wenzel, M. R. Wegewijs, and H. Schoeller, *Phys. Rev. Lett.* **90**, 076805 (2003).
- ¹² D. V. Cardamone, C. A. Stafford, and S. Mazumdar, *Nano Lett.* **6**, 2422 (2006).
- ¹³ A. Gagliardi, G. C. Solomon, A. Pecchia, T. Frauenheim, A. Di Carlo, N. S. Hush, and J. R. Reimers, *Phys. Rev. B* **75**, 174306 (2007).
- ¹⁴ W. Barford, *Electronic and Optical Properties of Conjugated Polymers* (Clarendon Press, Oxford, 2005).
- ¹⁵ A. Donarini, M. Grifoni, and K. Richter, *Phys. Rev. Lett.* **97**, 166801 (2006).
- ¹⁶ L. Mayrhofer and M. Grifoni, *Eur. Phys. J. B* **56**, 107 (2007).
- ¹⁷ K. Blum, *Density Matrix Theory and Applications* (Plenum, New York, 1996).